The LISA DFACS: Preliminary Model Predictive Control Design for the Test Mass Release Phase

IAC-20,C1,9,5,x58065

The LISA DFACS: Preliminary Model Predictive Control Design for the Test Mass Release Phase

S. Vidano[a]*, C. Novara[a], J. Grzymisch[b], M. Pagone[a]

[a] *Department of Electronics and Telecommunications, Politecnico di Torino, Corso Duca degli Abruzzi 24, 10129 Torino, Italy,* simone.vidano@polito.it
[b] *Guidance, Navigation and Control Section (TEC-SAG), ESTEC, European Space Agency, Kepleralaan 1, Noordwijk 2201 AZ, The Netherlands.*
* Corresponding Author

Abstract

This paper presents a preliminary control design for the test mass release phase of the LISA space mission. LISA will feature a triangular constellation of three spacecraft dedicated to the detection of gravitational waves. Each spacecraft carries two cubic free-falling test masses needed for the scientific experiment, which are initially locked by a clamp mechanism. When the plungers are retracted, the free-floating test masses are captured electrostatically by means of an electrostatic suspension system. However, the low actuation authority and the critical initial conditions, make the attitude and translation control of the test mass a difficult task. Model Predictive Control (MPC) appears to be a suitable technique for this application because of its ability to deal with the state constraints and the input saturations. In the present paper, the TM release context is briefly analysed, then the preliminary MPC design and simulation results are shown.

Keywords: LISA, MPC, control, spacecraft, GNC

Nomenclature

Scalars: $a, b \in \mathbb{R}$.

Column vectors: $\mathbf{r} = (r_1, \dots, r_n) = [r_1 \ \dots \ r_n]^T \in \mathbb{R}^{n\times 1}$

Row vectors: $\mathbf{r}^T = [r_1 \ \dots \ r_n] \in \mathbb{R}^{1\times n}$

Null vectors: $\mathbf{r} = \mathbf{0}$

Matrices: $M \in \mathbb{R}^{n\times m}$

Acronyms/Abbreviations

CoM	Center of Mass
DFACS	Drag Free and Attitude Control System
DoF	Degree of Freedom
ERF	Electrical Reference Frame
GPRM	Grabbing, Positioning and Release Mechanism
GRS	Gravitational Reference Sensor
HR	High Resolution mode
LISA	Laser Interferometer Space Antenna
MRF	Mass Reference Frame
MPC	Model Predictive Control
MPS	Micro Propulsion System
OA	Optical Assembly
SC	Spacecraft
SRF	Spacecraft Reference Frame
TM	Test Mass
WR	Wide Range mode

1. Introduction

The LISA mission will feature a triangular constellation of three spacecraft dedicated to the detection of gravitational waves in the 0.2 mHz – 1 Hz bandwidth. Each spacecraft carries two cubic free-falling test masses, that play a fundamental role in the scientific experiment [1].

These test masses are located inside an advanced electrostatic suspension system called the Gravitational Reference Sensor (GRS) [2, [3]. To withstand the high forces and vibrations at launch, they are initially locked by a clamp mechanism [4]. A Grabbing, Positioning and Release Mechanism (GPRM) is used to release the test masses inside the GRS. During the release phase, a set of plungers are retracted, and the electrostatic suspension must capture the test mass, despite a low actuation authority of about 1 μN and 10 nNm.

The GPRM was already tested in flight by the technological demonstrator LISA Pathfinder in 2016 [5], obtaining a release performance worse than expected. Due to the high initial velocities, the test masses hit the plungers and the GRS walls [5]. After losing part of their kinetic energy, the sliding mode controllers were able to capture the test masses by means of the electrostatic suspensions [5].

In the present work, Model Predictive Control (MPC) is applied to the TM release control problem. Compared to the sliding mode developed for LISA Pathfinder [5, [6, [7], MPC is a different technique that provides optimal (eventually sub-optimal) command inputs by solving an

optimization problem online, which takes into account input saturations and constraints on states. This has the potential of utilizing to the full extent the available control authority, potentially maximizing the chances of successful electrostatic capture. Moreover, the present MPC was designed to cope with the in-flight initial conditions experienced by LISA Pathfinder.

In the present paper, the plant is briefly described. Then the MPC design is presented and preliminary simulation results are shown.

2. Methodology

In the present work, an MPC [8] controller was designed to control the attitude and translation of the test mass after its release. The nonlinear model of the TM dynamics [9] was used to set up a simulation environment in Matlab-Simulink. Then it was linearized obtaining the internal prediction model of the MPC. The cost function was defined, and the problem constraints were set according to the characteristics of the actuators and sensors. Finally, the controller was implemented with the MPC toolbox and tested in simulation.

3. Control Design

1.1 Plant Description

The spacecraft concept (see Fig. 1) consists of a science module that carries two moving Optical Assemblies (OA) whose nominal inter-angle is 60°. Each OA consists of a telescope, an optical bench for laser interferometry and a vacuum electrostatic suspension system (the Gravitational Reference Sensor), which houses a suspended cubic test mass (TM) [2]. A GPRM system of movable plungers is used to release the test masses, thus leaving them free-floating inside the GRS. A single LISA spacecraft is therefore a multi-body system characterized by 20 degrees of freedom: 6 DoFs for the spacecraft platform, 1 DoF for each optical assembly, 6 DoFs for each test mass.

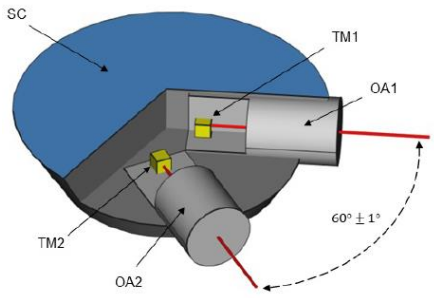

Fig. 1. LISA spacecraft

The test mass degrees of freedom can be measured and controlled at the same time by means of the GRS (see Fig. 2). This device is composed of a vacuum chamber, an electrode housing, passive and active mitigation systems for the local disturbances and the locking mechanism [10]. The whole GRS was tested in-flight by LISA Pathfinder and will be inherited by LISA.

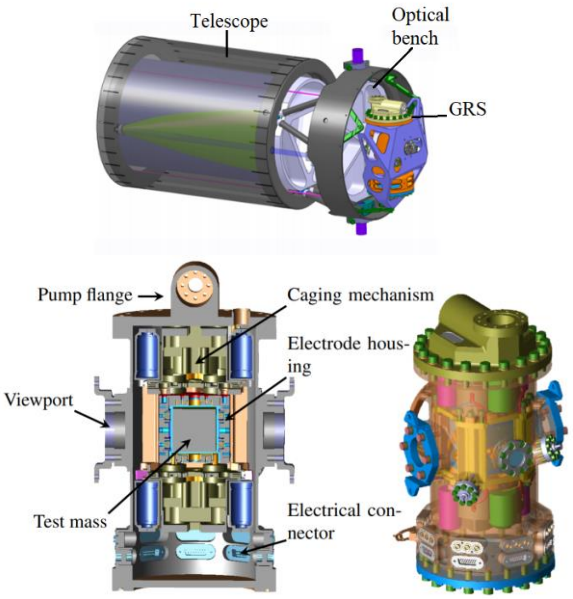

Fig. 2. Optical Assembly and GRS [2]

Three different issues affect the control problem: i) low actuation authority, ii) critical initial conditions, iii) TM stiffness.

The electrostatic suspension of the GRS is composed of a set of electrodes of different dimensions due to mechanical accommodation constraints. The approximate force/torque authority is reported Table 1. Note that the force/torque authority is relatively low.

Table 1. GRS input saturation actuation features

	DoF	Wide Range Mode
Force saturation	x	1000 nN
	y	1000 nN
	z	600 nN
Torque Saturation	X	10 nNm
	Y	15 nNm
	Z	10 nNm

The second issue is related to the TM initial conditions. According to [5, [11], the plunger retraction provides to the test mass some initial conditions due to adhesion and force asymmetries. When the test masses were released in LISA Pathfinder, the initial conditions were higher than expected. According to [5], the highest initial conditions occurred on the lateral translation (-454.6 μm, -22.3 μm/s) and on the roll coordinate (15.4 mrad, 685 μrad/s). This was potentially due to an unexpected combination of mechanical tolerances and synchronization issues between the two sides of the release system.

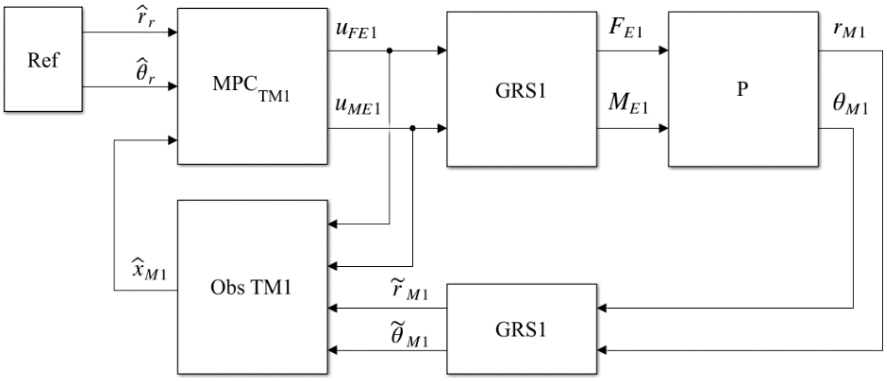

Fig. 3. Control architecture

One last characteristic of the plant that affects the control is given by the TM stiffness. Even though the test mass is free floating inside the GRS after its release, the interactions with the spacecraft gravitational and electromagnetic fields generate some disturbance forces and torques ($\boldsymbol{F_S}$, $\boldsymbol{M_S}$) that are proportional to the test mass displacement and attitude [12, [13, [14] with respect to the cage center. These disturbances are modelled as a system of virtual springs (1) [12, [13, [14] and the main consequence is that they generate cross couplings between all the degrees of freedom of the test mass.

Two reference frames can be defined for the TM release control problem

- the Electrostatic Reference Frame (ERF) centred on the cage centre of the GRS, the x-axis is parallel to the telescope symmetry axis and the z-axis is parallel to that one of the spacecraft frame;
- the Mass Reference Frame (MRF) centred on the test mass CoM. The axes are perpendicular to the cube's faces.

The control objectives are to place the TM CoM on the ORF origin and align the MRF with the ORF.

1.2 Control architecture

The control architecture adopted in the present work is shown in Fig.3 and consists of an MPC controller that provides the command force $\boldsymbol{u_{FE}}$ and the command torque $\boldsymbol{u_{ME}}$ to the actuator. The electrostatic suspension applies forces and torques to the test mass, whose position $\boldsymbol{r_M}$ and attitude $\boldsymbol{\theta_M}$ are measured by the GRS. A state observer provides the TM states estimate to the controller, which is used to initialize the internal prediction model of the MPC and filter the measurement noise.

In future work, the behavior of both the MPC controllers (one for each GRS) acting in parallel with the spacecraft attitude control will be studied.

1.3 MPC Design

The discrete MPC optimization problem was formulated as follows:

$$\min J$$

$$J = \sum_{K=1}^{N} \left[S_y^{-1}(\boldsymbol{y}_k - \boldsymbol{y}_r)^T Q(\boldsymbol{y}_k - \boldsymbol{y}_r) + S_u^{-1}(\boldsymbol{u}_k)^T R(\boldsymbol{u}_k) + \right. \\ \left. + S_{ur}^{-1}(\boldsymbol{u}_k - \boldsymbol{u}_{k-1})^T R_{ur}(\boldsymbol{u}_k - \boldsymbol{u}_{k-1}) \right] \tag{1}$$

subject to

$$\begin{aligned} \boldsymbol{x}_{k+1} &= A\boldsymbol{x}_k + B\boldsymbol{u}_k \\ \boldsymbol{y_k} &= C\boldsymbol{x}_k + D\boldsymbol{u}_k \end{aligned} \tag{2}$$

$$-\boldsymbol{c_r} \le \boldsymbol{y}_k \le \boldsymbol{c_r} \tag{3}$$

$$-\bar{\boldsymbol{u}} \le \boldsymbol{u}_k = \begin{bmatrix} \boldsymbol{F}_E \\ \boldsymbol{M}_E \end{bmatrix} \le \bar{\boldsymbol{u}} \tag{4}$$

where k is the prediction step, N is the prediction horizon, $\boldsymbol{u}_k$ is the k-th input vector, $\boldsymbol{y}_k = (\boldsymbol{r}_{Mk} \quad \boldsymbol{\vartheta}_{Mk})$ is the k-th output vector, $\boldsymbol{y}_r = (\boldsymbol{r}_r \quad \boldsymbol{\vartheta}_r) = \boldsymbol{0} \quad \forall\, k \ge 0$ is the reference vector. The cost function (2) minimizes the norm of the output error, the norm of the control input $\boldsymbol{u_k}$ and its rate. Q, R, R_{ur} are diagonal weighting matrices, $S_y^{-1}, S_u^{-1}, S_{ur}^{-1}$ are scaling factor matrices.

The internal state space model (2) is needed to predict the states up to the prediction horizon N and the outputs are used to compute the cost function. It was obtained by linearizing the nonlinear system around the settling point $(\boldsymbol{r}_M \quad \boldsymbol{\vartheta}_M) = \boldsymbol{0}$. To perform predictions, the state space model (2) needs to be initialized. Hence, a Kalman filter was used to find a state estimate and initialize (2). Constraints (3) and (4) are related to the input saturations and the GRS sensing range. The controller sampling time was set to $T_S = 0.10$ s (10Hz), which is the update rate of the electrostatic suspension. The prediction horizon N was set to 100 T_S to improve performance and the control horizon C was set to 1 T_S to have a faster algorithm.

4. Results

The MPC controller was tested in a reduced simulation environment including:

- Constant disturbances and TM stiffness.
- Local environmental noises (force and torque noises acting on the test mass).
- Actuation and sensing noises of the electrostatic suspension.

The initial conditions of the test mass are those of LISA PF [5]. The references are $\boldsymbol{y_r = 0}$ because with want to reach the cage centre with the same orientation of the optical frame.

Fig. 4 and Fig. 5 show that the test mass states reach the null reference as expected. At the beginning, the test mass is quickly moving away from the cage centre due to the large initial conditions. Consequently, the MPC predicts this behaviour and reacts by applying the maximum forces and torques. Once the test mass is slowed down, it is positioned back to the cage centre with minimized control forces and torques. The controller was able to capture the test mass even starting from the bad initial conditions of LISA Pathfinder occurred in-flight. The sensing range constraints were not violated. Anyway, an average steady state error of $1 \cdot 10^{-5}$ m occurred on the test mass translation and $6 \cdot 10^{-6}$ rad on the attitude. This was related to the parameters of the measurement noise model in the Kalman filter. Indeed, by adjusting the parameters it was possible to obtain a lower steady state error of about $5 \cdot 10^{-7}$ on all the output variables, but on the other hand, a second-order like transient with more oscillations was obtained.

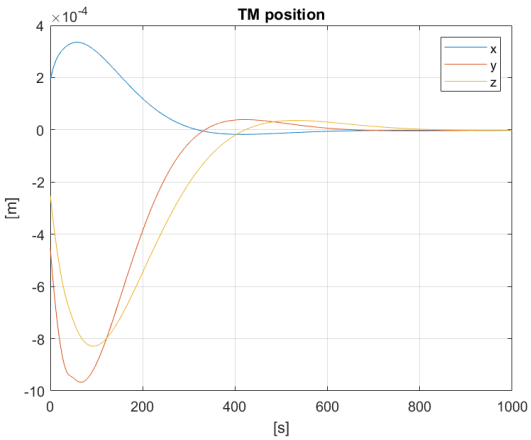

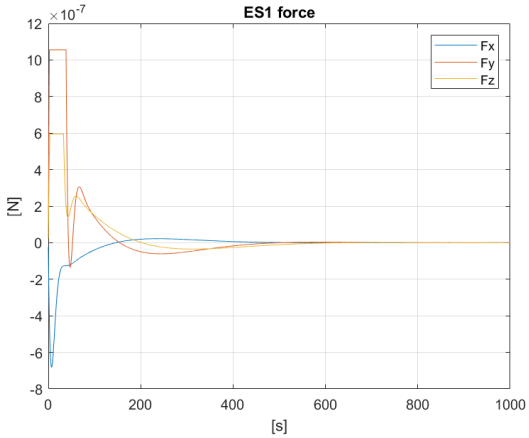

Fig. 4. TM position and attitude

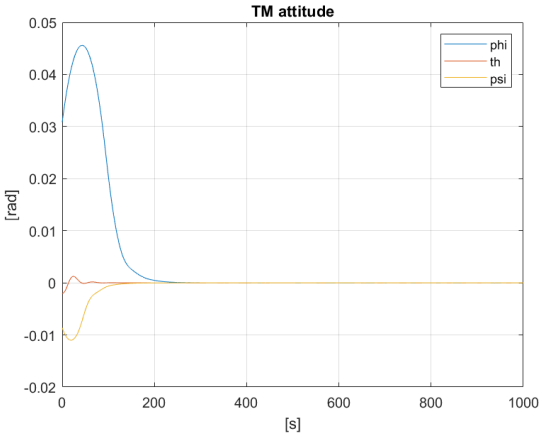

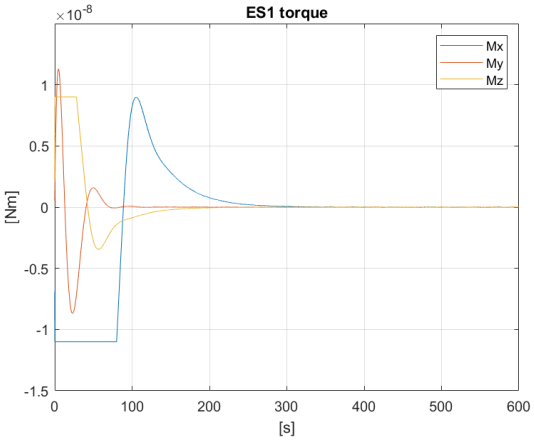

Fig. 5. Command forces and torques of the GRS

6.

Conclusions

The test mass release control problem of the LISA mission has been tackled in this paper, using a more advanced control technique than in LISA Pathfinder. The plunger retraction of the locking mechanism provides to the test mass large initial condition, as experienced by LISA Pathfinder in-flight. Together with the low actuation authority and the TM stiffness disturbances, this makes the electrostatic capture a difficult task.

An MPC controller was designed and preliminary simulation results show satisfactory performance. The controller was able to capture the test mass even starting from the LISA Pathfinder initial conditions. However, a steady state error of $1 \cdot 10^{-5}$ m on the translation coordinates was obtained, which could be too high when switching to the finer High-Resolution mode. This issue can be overcome with a finer tuning of the MPC parameters. In any case, according to the obtained results, it can be concluded that MPC is a suitable control technique for this application since it is a MIMO control that provides optimal/suboptimal commands in presence of constraints on states and inputs.

Future work should focus on the improvement of the steady state error, robustness evaluation by performing a Monte Carlo simulation campaign, and the design of an MPC that works in parallel with the spacecraft attitude control loop and solar pressure force compensation.

Acknowledgements

The present work was supported by ESA/ESTEC.

References

[1] P. Amaro-Seoane et al., Laser Interferometer Space Antenna, arXiv e-prints, p. arXiv:1702.00786, Feb 2017.

[2] ESA, LISA Yellow Book, Assessment Study Report, 2011.

[3] M. Sallusti et al., LISA system design highlights, *Class. Quantum Grav.* 26 094015, 2009.

[4] C. Zanoni et al., Summary of the results of the LISA-Pathfinder Test Mass release, Journal of Physics: Conference Series. 610 012022, 2015.

[5] A. Schleicher et al., In-Orbit Performance of the LISA Pathfinder Drag Free and Attitude Control System, 10th International ESA GNC Conference, 2017.

[6] F. Montemurro et al., Control Design of the Test Mass Release Mode for the LISA Pathfinder Mission, AIP Conference Proceedings 873 583, 2006.

[7] F. Montemurro et al., Sliding Mode Technique Applied to the Test Mass Suspension Control, IFAC Proceedings Volumes, Volume 40, Issue 7, pp. 627-632, 2007.

[8] E. Camacho and C. Bordons Alba, Model Predictive Control, Springer, 2007.

[9] S.Vidano et al., The LISA DFACS: a Nonlinear Model for the Spacecraft Dynamics, Aerospace Science and Technology, 2020.

[10] O. Jennrich, LISA Technology and Instrumentation, Classical and Quantum Gravity, 2009. doi 10.1088/0264-9381/26/15/153001.

[11] D. Bortoluzzi et al. On-ground testing of the role of adhesion in the LISA-Pathfinder test mass injection phase, Advances in Space Research 59, 2017.

[12] D. Gerardi, Advanced drag-free concepts for future space-based interferometers: acceleration noise performance, Review of Scientific Instruments 85, 011301, 2014.

[13] S. Merkowitz, Self-Gravity modelling for LISA, Classical and Quantum Gravity 22, pp.395-402, 2005.

[14] T. Ziegler, Test Mass Stiffness Estimation for the LISA Pathfinder Drag-Free System, AIAA GNC Conference and Exhibits, 2007.